Available online at www.sciencedirect.com

ScienceDirect

journal homepage: http://www.elsevier.com/locate/rpor

Original research article

# Evaluation of application of EPID for rapid QC testing of linear accelerator

*Shahla Ebrahimi Moghadam, Shahrokh Nasseri, Seyedeh Somayeh Seyedi, Hamid Gholamhosseinian, Mehdi Momennezhad**

*Department of Medical Physics, Faculty of Medicine, Medical Physics Research Center, Mashhad University of Medical Sciences, Mashhad, Iran*

ARTICLE INFO

*Article history:*
Received 12 June 2017
Received in revised form
15 May 2018
Accepted 21 July 2018
Available online 13 August 2018

*Keywords:*
Linear accelerator
Quality control
EPID

ABSTRACT

*Aim:* Evaluation of application of EPID for rapid QC testing of linear accelerator.
*Background:* Quality control of a linear accelerator device is a time and energy intensive process. In this study, attempts have been made to perform the linear accelerator quality control using electronic portal imaging device (EPID), which is mounted on most accelerators.
*Materials and methods:* First, quality control and dosimetry parameters of the device were determined and measured based on standard protocols to ensure full calibration of the accelerator. Then, various features of EPID including spatial resolution and contrast resolution, the effect of buildup region, dose response and image uniformity were evaluated. In the next step, consistent with the parameters of linear accelerator quality control including field size, field flatness and symmetry, the light field coincidence with X-ray field, mechanical stability and multileaf collimator position accuracy test, the output images of device were obtained.

After feeding images to the MATLAB software, their pixel content was analyzed. All measurements of the three photon beams were repeated three times.
*Results:* The EPID image had a desirable resolution, contrast and uniformity and displayed high sensitivity to dose changes with linear dose response. Seven qualitative parameters of the linear accelerator were then controlled by EPID.
*Conclusions:* The results of the linear accelerator quality control using the EPID were consistent with practice. Quality control using the EPID was more convenient and faster than conventional methods.
© 2018 Greater Poland Cancer Centre. Published by Elsevier Sp. z o.o. All rights reserved.

* *Corresponding author.*
E-mail address: momennezhadm@mums.ac.ir (M. Momennezhad).
https://doi.org/10.1016/j.rpor.2018.07.008
1507-1367/© 2018 Greater Poland Cancer Centre. Published by Elsevier Sp. z o.o. All rights reserved.

## 1. Background

Radiation therapy is a multistep process. To ensure treatment quality and accurate dose delivery, each step has its unique standards and quality control programs. One of the equipment used to enhance the precision of the treatment is EPID which is composed of a two-dimensional array of small dosimeters that are capable of acquiring images of megavoltage radiation beams. The system output is a digital image of DICOM format and its pixel content can be analyzed. The main application of these systems is to control the position of the patient and the treatment area prior to radiation therapy by means of imaging and comparing images with the reference digital reconstructed radiograph image (DRR).[1]

In recent years, the utilization of EPID images to perform quality control test for linear accelerator devices,[2,3] evaluate the performance of multileaf collimator[4,5] and dose distribution in the treatment area[6,7] have been investigated in a growing number of studies.

## 2. Aim

Since quality control tests and dosimetry of linear accelerator devices based on standard protocols, such as AAPM (TG 51) protocol,[8] is time consuming and requires prolonged exposure time and use of special equipment, such as a water phantom and various dosimeters, this study was designed to explore the application of EPID for rapid quality control testing of accelerators.

## 3. Materials and methods

In this study, Elekta linear accelerator (Precise model) was used. The device is equipped with multileaf collimators consisting of 80 leaves (the leaf width in the isocenter is 1 cm) and electronic portal imaging device. In the photon mode, there are three energy (8, 10 and 15 MV) and in the electron mode there are five energy (6, 8, 10, 15 and 18 MeV) states. The linear accelerator calibration was performed according to AAPM (TG-51) protocol.[8]

Distance between the source and the detector was fixed (157 cm). The light sensitive layer had $1024 \times 1024$ pixels with a pixel size of $0.4 \times 0.4\,mm^2$. Thus, the EPID size was $409.6 \times 409.6\,mm^2$. Each pixel was 0.25 mm in isocenter with a maximum imaging field of $25.9 \times 25.9\,cm^2$ in the isocenter. In this paper, all measurements except for dose linearity test, were performed at 10 MU with a dose rate of 400 MU/min. Before any measurement, equipment was calibrated to increase the accuracy of calculations and allows comparison of measurements. To confirm the reproducibility, each measurement was repeated 3 times. Images were analyzed in MATLAB software (Ver 2014Ra) using image processing toolbox to implement M-file functions and then graphical user interface toolbox to facilitate quality control testing.

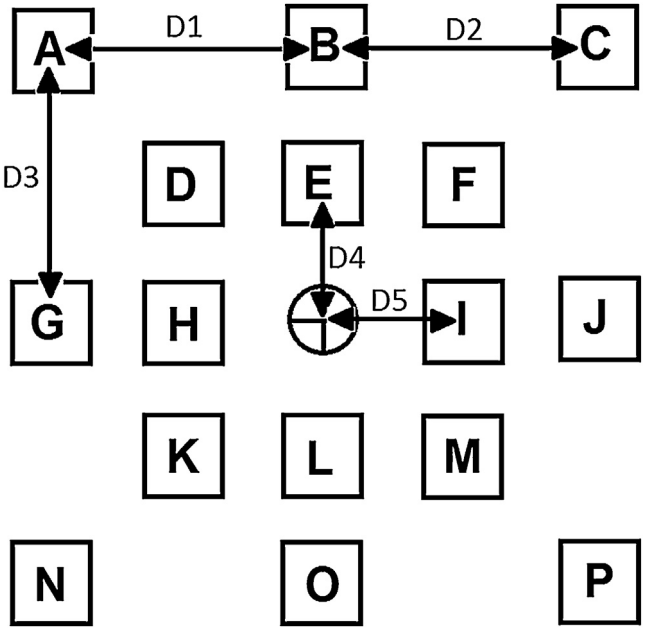


**Fig. 1 – The selected area to check uniformity.**

### 3.1. *Image quality*

To determine the spatial resolution and contrast resolution, the Las Vegas Phantom was placed on the treatment table and the irradiation was performed at SSD = 100 cm and field size = $15 \times 15\,cm^2$. The quality of the images was evaluated according to AAPM TG-58.[9] This process was carried out for all three photon energies.

### 3.2. *Dose linearity*

Dose linearity of linear accelerator was verified using scanditronix wellhofer dosimetry system including water phantom and Farmer ion chamber. To check the dose response linearity of EPID, images were captured in an open field of $10 \times 10\,cm^2$ with monitor units of 10, 20, 50, 100 and 150 at dose rates of 200 MU/min and 400 MU/min. The average value of pixels in a $40 \times 40$ pixel square at the center of each image was obtained. Pixel value versus MU was plotted. This test was conducted for 6, 10 and 15 MV energies as well.

### 3.3. *Pixel uniformity response*

EPID system calibrates images using Flood Field (FF) and Dark Field (DF) images. This removes the off axis effect and bad pixels and produces image uniformity. However, it is necessary to evaluate the image uniformity. For this purpose, using the method proposed by Kavuma et al.,[10] images with a field size of $20 \times 20\,cm^2$ were prepared for three photon energies of 6, 10 and 15 MV. According to Fig. 1, in 16 regions and center of the image, squares with a pixel size of $40 \times 40$ were selected and then a comparison was drawn between average pixel count in all 16 regions and average pixel count at the center. D1_D2 and D3_D4 distances were 7 cm and D4_D5 were 4 cm.

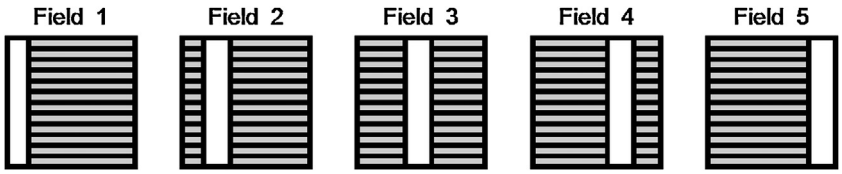


**Fig. 2 – Schematic view of fields of picket fence test.**

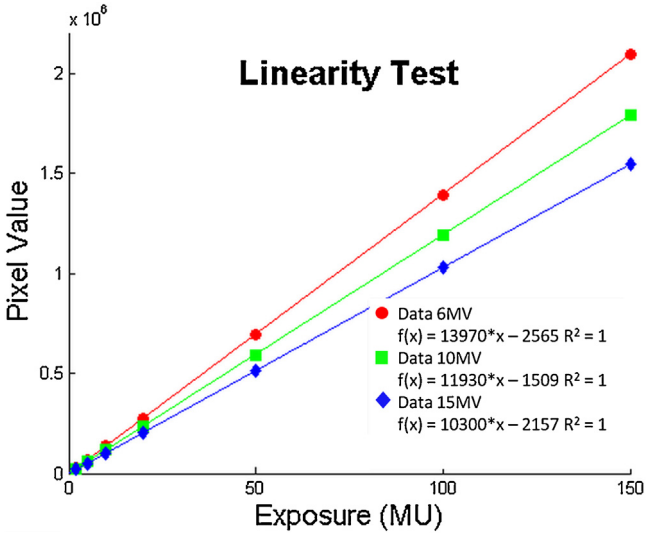


**Fig. 3 – EPID linear response to MU.**

### 3.4. *Build-up layer measurements*

By removing the treatment table from the beam path, solid water equivalent phantom layers with a layer thicknesses of 0, 2, 5, 7, 9, 12, 15, 17, 20 and 22 mm in a field of $10 \times 10\,cm^2$ and energy of 6 MV were placed on EPID surface and irradiation was initiated. Average pixel values in a square of $40 \times 40$ pixels at the center of each image was obtained and the curve of pixel value versus phantom thickness was plotted.

For energies of 10 and 15 MV, a layer thickness of 0, 2, 5, 7, 9, 12, 15, 17, 20, 22, 25 and 30 mm was selected.

### 3.5. *Field size, flatness and symmetry*

Two open fields of $10 \times 10\,cm^2$ and $20 \times 20\,cm^2$ at zero angles of collimator and gantry were imaged for three photon energies. Then, the field profile was drawn in the in-plane and cross-plane directions. Field edges were defined by 50% of the dose at the center of the field and the field size was calculated.

Flatness and symmetry of the field were measured both in reference zone by defining 80% of the field size and in the in-plane and cross-plane directions in accordance with IEC (International Electrotechnical Commission)[11] using the following formulas.

$$\text{Flatness} = \left(\frac{D_{max}}{D_{min}}\right) \times 100 \quad (1)$$

$$\text{Symmetry} = \left(\frac{D_{left}}{D_{right}}\right) \times 100 \quad (2)$$

In this relation, $D_{max}$ and $D_{min}$ were the largest and smallest pixel values in the reference zone, respectively. And $D_{left}/D_{right}$ represents the ratio of pixel values of two points which remain symmetric relative to the central axis at the reference zone.

Furthermore, flatness and symmetry was measured in the cross-plane and in-plane directions using water phantom and ion chamber in the field of $20 \times 20\,cm^2$.

### 3.6. *Coincidence of the light field and the X-ray field*

First, using the method proposed by Halabi et al.,[12] graticule alignment relative to the collimator axis of rotation was investigated. The field was opened asymmetrically along the X2 and Y1 (10 cm), and along X1 and Y2 (0.3 cm). The exposure was done in a double expose mode at the zero angle of collimator and gantry. The collimator was rotated 180 degrees and irradiation was repeated. The central point was irradiated twice. The center points were identified, and a straight line was drawn across the points that were in the same direction.

To examine the coincidence of light field and the X-ray field, a field of $10 \times 10\,cm^2$ was opened at SSD = 100 cm and collimator and gantry angles of zero. Using graph paper and shadow of graticule points, the accuracy of the light field was verified. Then, in the double expose mode with a field of $10 \times 10\,cm^2$ and $15 \times 15\,cm^2$, successive images were captured. The deviation between the edge of the $10 \times 10\,cm^2$ field and the center of points in the image was achieved.

### 3.7. *Mechanical stability*

With an open field of $10 \times 10\,cm^2$, zero collimator angle and gantry angles of 0–315 degrees at 45 degree intervals, the image was obtained. The difference between EPID matrix center and the field center was computed in the cross-plane and in-plane directions.

### 3.8. *MLC leaf position accuracy*

The Picket Fence test was used to examine this factor. In this test, small fields of 1 mm are radiated at distances of several centimeters. Since the minimum distance between MLC leaf pairs produced by the Elekta Company is 1 cm, to do this test, first a field with a width of 51 mm and a height of 26 cm was created and then the field center was swept from −10 cm to +10 cm at an interval of 5 cm. The irradiation was repeated 5 times and 5 images were obtained. All images were captured

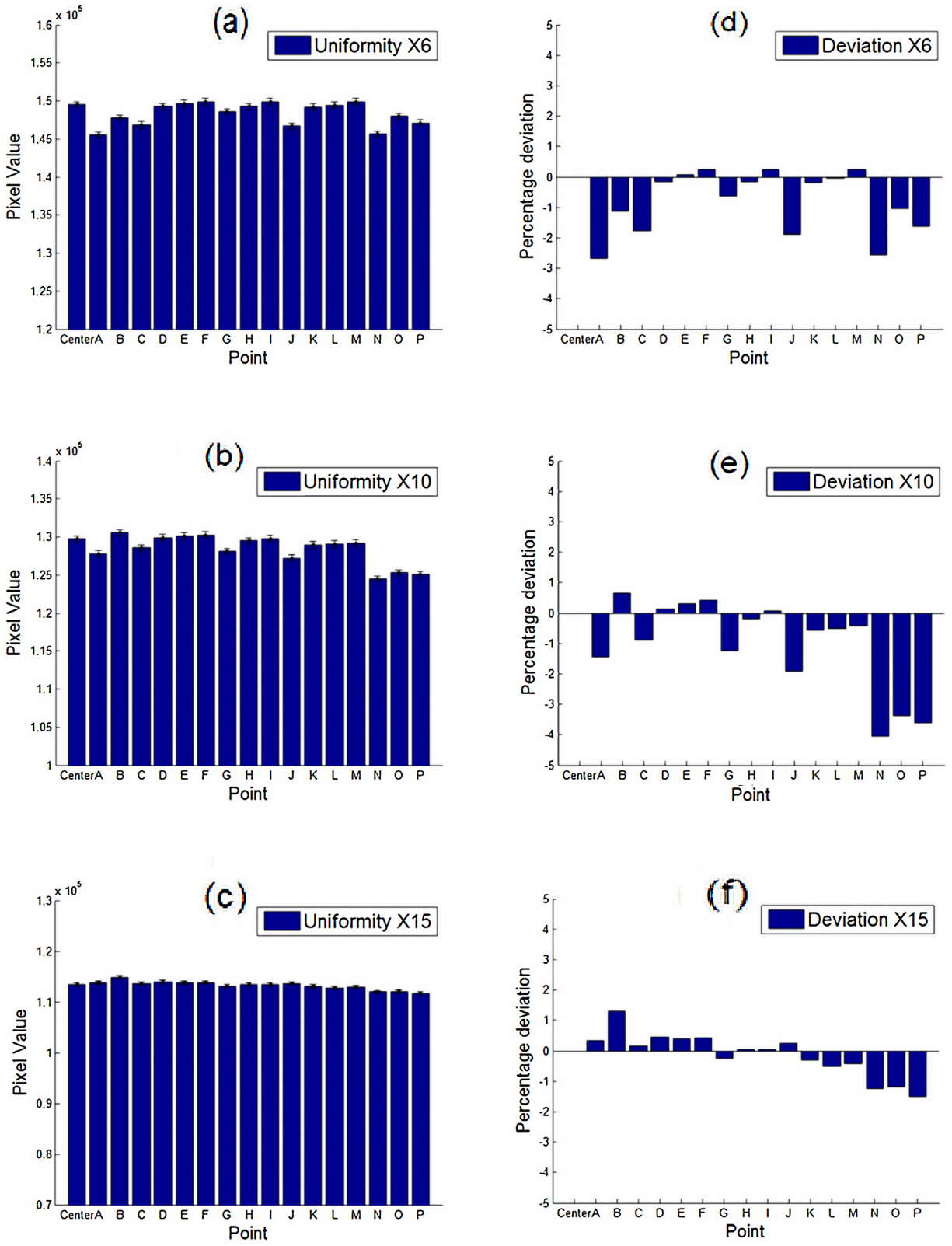


**Fig. 4 – The mean values of pixels and their differences relative to the central image pixels at 6(a, d), 10 (b, e) and 15(c, f) MV.**

by a 6 MV photon beam. Fig. 2 shows a schematic of the fields. The final image was the sum of 5 images, which depicted the radiated plane with 1 mm double irradiated strips.

To determine the position of each separate leaf, the cross plane profile was drawn from the site of each pair of leaves in the image. The peaks in the profile shows the gap center.

**Table 1 – The results of measuring the field size, flatness and symmetry for fields with nominal size 10 and 20 cm, in both directions of cross plane and in plane through EPID for energies of 6, 10 and 15 MV.**

| Energy | Nominal field size (cm) | Field size | | Flatness | | Symmetry | |
|---|---|---|---|---|---|---|---|
| | | In plane | Cross plane | In plane | Cross plane | In plane | Cross plane |
| 6 MV | 10 | 99.75 | 99.25 | 104.38 | 105.56 | 101.39 | 101.92 |
| | 20 | 200.08 | 199.00 | 103.32 | 104.41 | 101.43 | 102.46 |
| 10 MV | 10 | 99.66 | 99.33 | 106.85 | 104.19 | 104.91 | 101.52 |
| | 20 | 200.08 | 199.25 | 107.43 | 104.11 | 105.63 | 101.55 |
| 15 MV | 10 | 99.50 | 99.25 | 106.43 | 103.31 | 103.69 | 101.43 |
| | 20 | 200.08 | 199.41 | 104.53 | 102.41 | 103.92 | 101.48 |

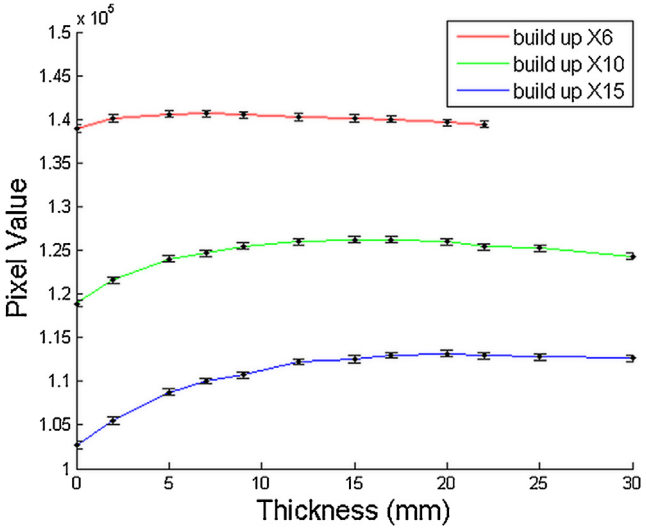


**Fig. 5 – EPID response to different thicknesses of build up layers for energies of 6, 10 and 15 MV.**

Each profile was the outcome of averaging three cross plane profiles and there were four peaks in each profile.

The position error was calculated for each pair of leaves based on the difference between the calculated and planed position. The histogram of results were plotted.

## 4. Results

**Image quality**: In the images derived from Las Vegas phantom at energies of 6, 10 and 15 MV 16, 13 and 11 holes were observed, respectively. Therefore, according to acceptance test guidelines quality of EPID images was desirable.

**Dose linearity**: Fig. 3 shows EPID response in terms of monitor unit. In the range of 2–150 MU, there was a linear relationship between EPID and monitor unit for all three photon energies at two different dose rates.

**Pixel uniformity response**: Results of measurement in 17 regions of a field of $20 \times 20\,cm^2$ are illustrated in Fig. 4. The pixel values for energies of 6, 10 and 15 MV are shown in Fig. 4(a)–(c), and the difference between pixel values and central pixels values are demonstrated in Fig. 4(d)–(f).

**Build-up effect**: as shown in Fig. 5, for an energy of 6 MV at EPID surface, there is no need for an additional build-up layer and for energies of 10 and 15 MV with a water equivalent thickness of 5 and 12 mm, the flat dose region was obtained.

**Field size, flatness and symmetry**: Field profiles with nominal dimensions of $10 \times 10\,cm^2$ and $20 \times 20\,cm^2$ in the cross-plane (AB) and in-plane (GT) directions are plotted in Fig. 6. Table 1 shows estimated values for the field size, flatness and symmetry for two square fields with nominal dimensions of 10 cm and 20 cm for energies of 6, 10 and 15 MV.

Measurements of flatness and symmetry using a water phantom and ion chamber were showed in Table 2. These values were well compatible with the results of EPID.

### 4.1. *Coincidence of light field and X-ray*

Fig. 7 shows the results of the graticule alignment. The difference in cross sections of X axes is:

$$\frac{1.4213 - 0.6350}{2} = 0.3931\,mm$$

Which indicates that graticule horizontal axis needs to be moved 0.3931 mm from the isocenter to the gantry. Similarly, the difference in Y-axes is:

$$\frac{0.8652 - (-0.1463)}{2} = 0.5058\,mm$$

Which shows that graticule vertical axis has to be moved 0.5058 mm to the right.

In the resultant images, to determine coincidence of light field with X-ray field, Fig. 8 was marked with software code of detection spots. Also, using edge detection algorithms, the edge of a nominal field of $10 \times 10\,cm^2$ was detected, as shown by green lines in the figure. The maximum distance between the point center and lines of field edge was less than 1 mm.

### 4.2. *Mechanical stability*

Fig. 9 shows mechanical stability in the cross-plane and in-plane directions. There was no in-plane deviation and the maximum cross-plane deviation was 0.125 mm. The accepted criteria in (AAPM)TG-142 is 1 mm.[13]

**MLC leaf position accuracy**: Fig. 10 shows the difference between obtained and planned position of the leaf. The maximum difference was under 1 mm with mean = 0.08 and SD = 0.35.

## 5. Discussion

**Dose linearity**: the linear relationship between dose and EPID response is one of the most important features of EPID discussed in other studies.[14,15]

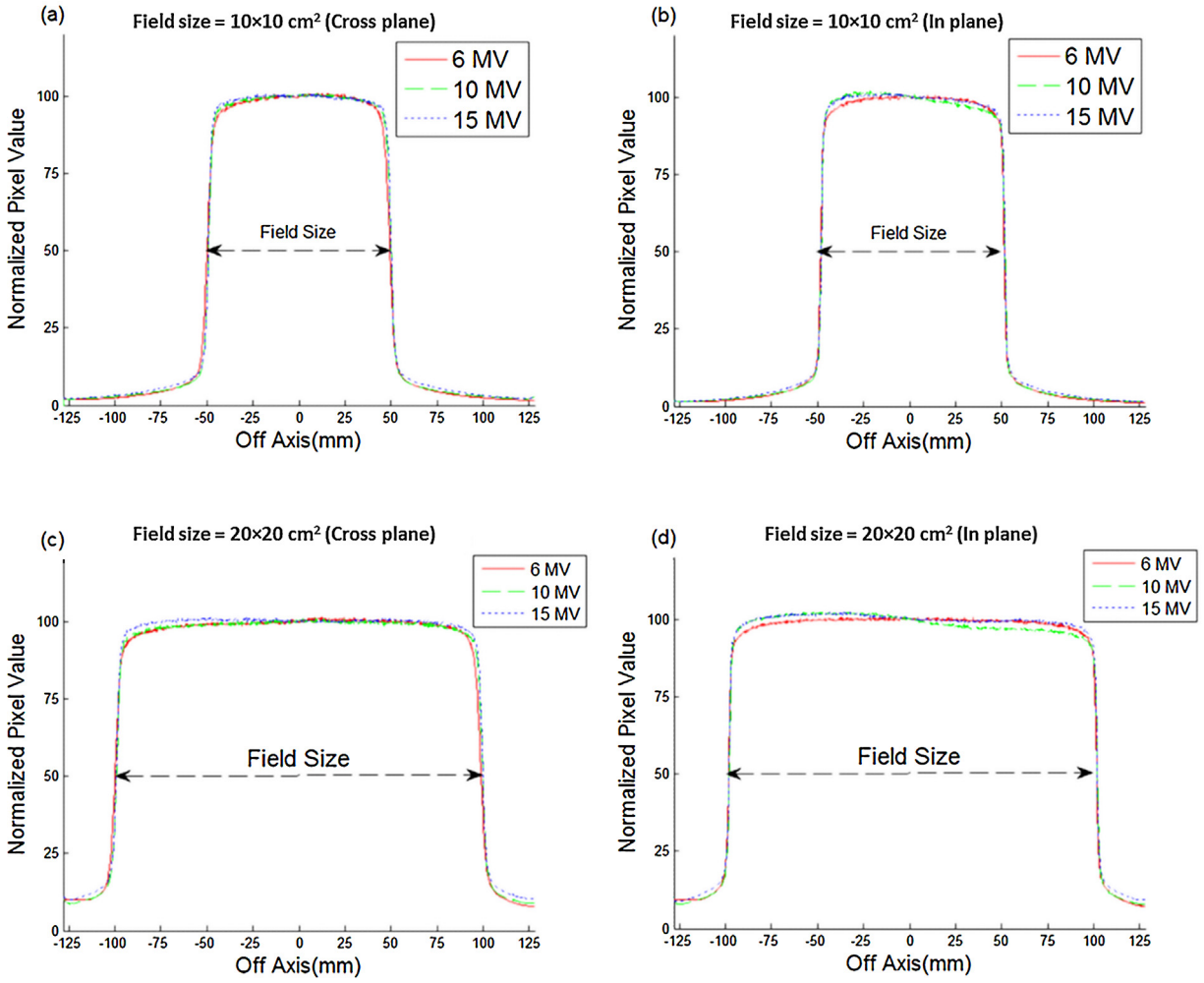


**Fig. 6 – A nominal field profile of 10 x 10 cm$^2$ at (a) cross plane (AB) and (b) in plane (GT) directions and a nominal field profile of 20 x 20 cm$^2$ at (c) cross plane (AB) and (d) in plane (GT) for all three energies.**

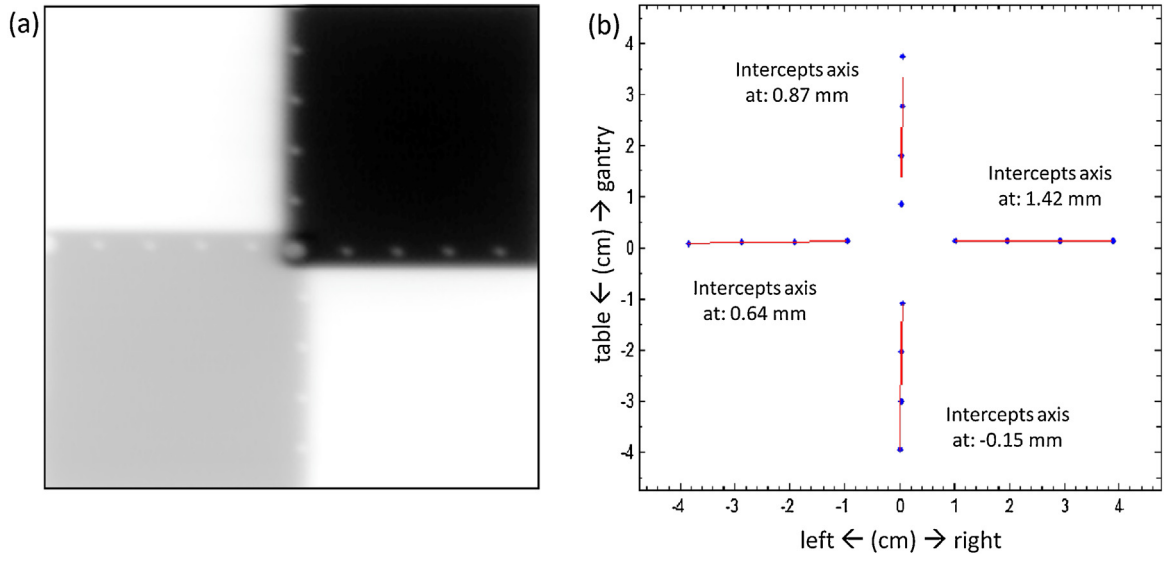


**Fig. 7 – Graticule alignment relative to the collimator rotation axes: (a) images generated by double exposure and (b) analysis of graticule misalignment relative to axes of collimator rotation.**

**Table 2 – The results of measuring the flatness and symmetry for field with nominal size 20 cm, in both directions of cross plane and in plane through water phantom and ion chamber for energies of 6, 10 and 15 MV.**

| Energy | Nominal field size (cm) | Flatness | | Symmetry | |
|---|---|---|---|---|---|
| | | In plane | Cross plane | In plane | Cross plane |
| 6 MV | 20 | 103.50 | 103.60 | 103.50 | 101.10 |
| 10 MV | 20 | 107.00 | 103.40 | 104.10 | 101.40 |
| 15 MV | 20 | 103.20 | 102.80 | 102.30 | 100.80 |

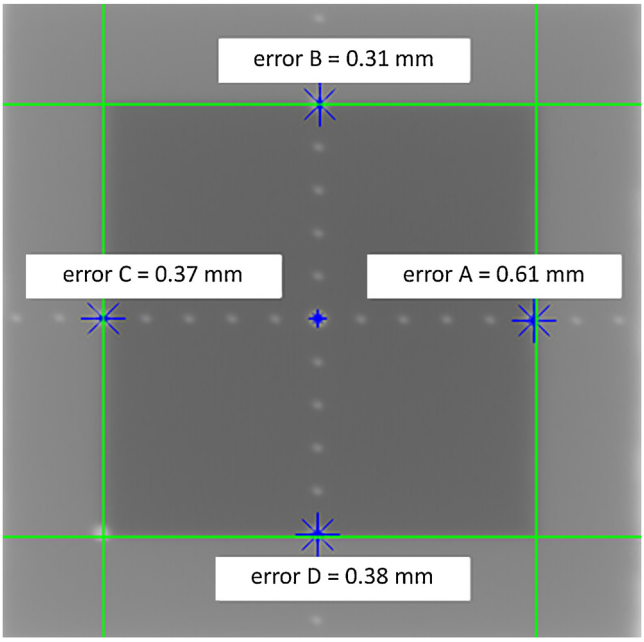


**Fig. 8 – Analyzing the coincidence of light field and X-ray by identifying field edges and center of graticule points and computing their difference.**

**Build up effect**: although measurement in areas with large dose variations is not strictly standard, the adoption of build-up layers makes measurements more complicated and difficult, and measurement possibility is limited to the zero angle for the gantry. Also, since conditions are identical for all measurements, removing an additional build-up layer from EPID does not affect the results of the project. Thus, in this study, an additional build-up layer was not used on EPID.

In previous studies on a variety of EPID systems, different results have been reported.

Winkler et al. proposed 1.5 mm copper thickness for EPID iViewGT model at energies of 6 and 10 MV and of 3 mm thickness at energies of 25 MV as additional build up materials on an EPID layer.[16]

Tyler et al. studied two different EPIDs, an iViewGT model of Elekta accelerator and an OptiVuel model of Siemens accelerator. They reported that in both models, to create electron balance at an energy of 10 MV, a 1 cm solid water phantom was needed as an extra layer, but for an energy of 6 MV, no build up was required.[17]

**Pixel uniformity response**: The results showed that the maximum difference between pixels in 16 regions of the image with a field center was less than 4.05%. Greer studied two EPIDs and reported a 5% difference.[18] Kavuma et al. studied 11 different EPIDs and reported a maximum deviation of 4.5%.[10] Our results are consistent with the literature.

**Field size, flatness and symmetry**: the field profile for energies of 10 and 15 MV along the cross-plane (AB) is flatter and more symmetrical than that of the in-plane (GT). This is probably due to the scatter caused by device arm and treatment table along the in-plane (GT) direction.

For an energy of 6 MV, profiles are similar and close in two directions, and no significant difference was observed.

The highest flatness value was 108.54, which was less than the criteria proposed by IEC (110).[11] As a result, dose had desirable uniformity in the radiation field.

The highest field symmetry value was 106.00. This value can be further reduced by using smoothing filters.

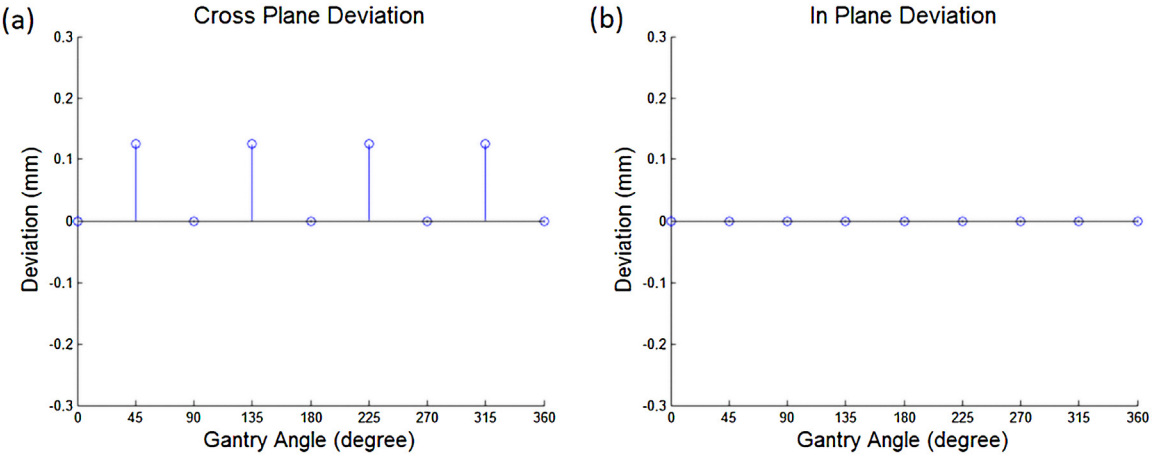


**Fig. 9 – Distance between center of open field 10 × 10 cm$^2$ and that of EPID matrix, in angle range from 0 to 360 degrees with angle interval 45 degrees in both cross line and inline directions.**

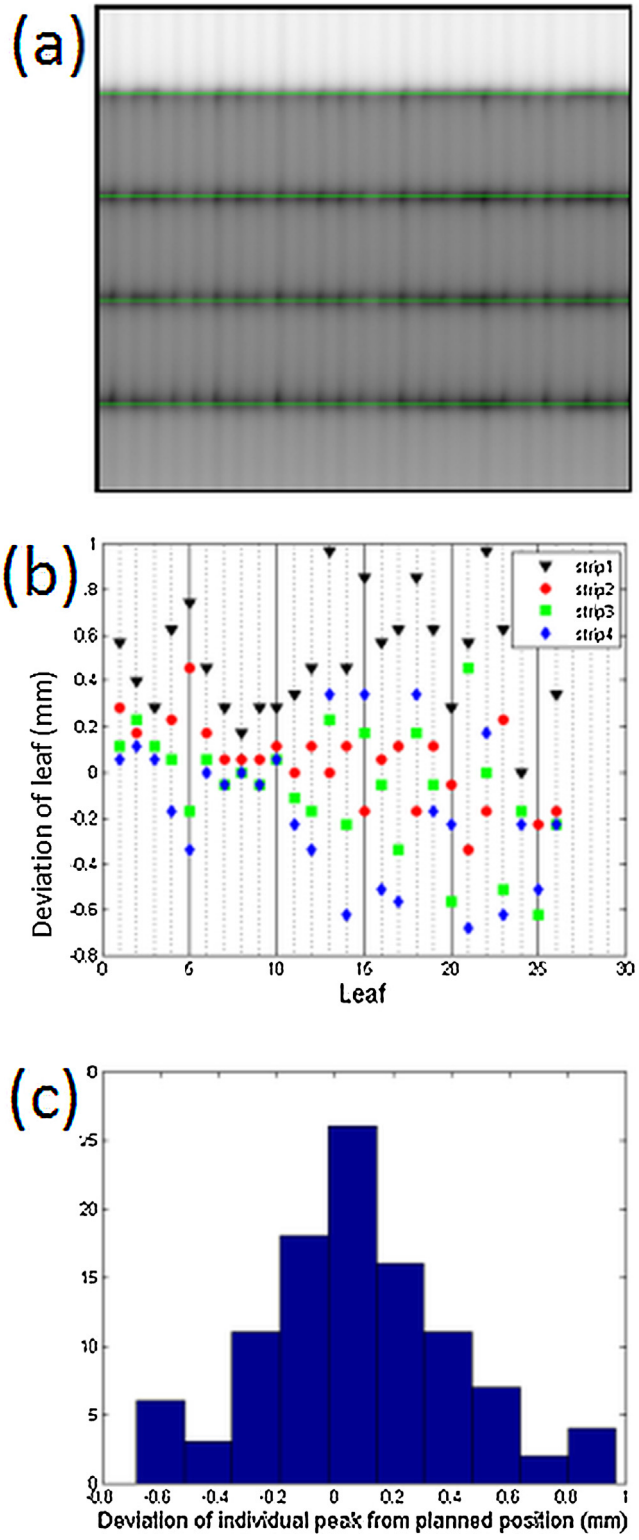


**Fig. 10 – Picket fence pattern and planned position (a), deviation of individual leaf (b), and histogram of deviations (c).**

### 5.1. *Coincidence of light field and X-ray field*

The difference between the center of dots and field edge was less than 0.7 mm. Given that a limit of 2 mm or 1% in both directions had been determined[13], the light field and X-ray field has desirable coincidence.

### 5.2. *MLC leaf position accuracy*

According to TG142,[13] the tolerance of spatial accuracy of leaves was 2 mm for non-IMRT and 1 mm for IMRT technique in all four gantry angles. Therefore, our result meets the AAPM TG 142 tolerance.

Sumida et al, investigated the position error for a multileaf collimator at 4 angles using the picket fence test. In this study, deviation of leaf position from the planned position was less than 1 mm and the average deviation was less than 0.5 mm.[13]

In the study of Anna Fredh et al., the position accuracy of 3 multileaf collimators was examined by EPID based on the picket fence test and a maximum deviation of 0.46 mm was achieved.[19]

## 6. Conclusions

In this study, the quality control for the EPID was carried out and then some parameters of quality control related to linear accelerator were explored using EPID. The results of EPID were in agreement with the practical method. Also, the quality control of MLC leaf position with the EPID was discussed.

In conclusion, EPID was found to be a suitable device for daily quality control of a linear accelerator. The quality control of a linear accelerator by EPID is faster with lower monitor unit consumption and reduced the depreciation of the linear accelerator.

## Conflict of interest

None declared.

## Financial disclosure

This survey was supported by Mashhad University of Medical Sciences. Results described in this report were part of MSc thesis.

## Acknowledgments

This survey was supported by Mashhad University of Medical Sciences. Results described in this report were part of MSc thesis.

REFERENCES

1. Van Elmpt W, McDermott L, Nijsten S, Wendling M, Lambin P, Mijnheer B. A literature review of electronic portal imaging for radiotherapy dosimetry. *Radiother Oncol* 2008;**88**(3):289–309.

2. Budgell GJ, Zhang R, Mackay RI. Daily monitoring of linear accelerator beam parameters using an amorphous silicon EPID. *Phys Med Biol* 2007;**52**(6):1721.
3. Sun B, Goddu SM, Yaddanapudi S, et al. Daily QA of linear accelerators using only EPID and OBI. *Med Phys* 2015;**42**(10):5584–94.
4. Kang D, Deng X, Huang S. Quality control for multileaf collimator leaf position accuracy using amorphous silicon electronic portal imaging devices. *Ai Zheng* 2009;**28**(7):771–4.
5. Sumida I, Yamaguchi H, Kizaki H, et al. Quality assurance of MLC leaf position accuracy and relative dose effect at the MLC abutment region using an electronic portal imaging device. *J Radiat Res* 2012:rrs038.
6. Celi S, Costa E, Wessels C, Mazal A, Fourquet A, Francois P. EPID based in vivo dosimetry system: clinical experience and results. *J Appl Clin Med Phys* 2016;**17**(3).
7. Mijnheer B, Olaciregui-Ruiz I, Rozendaal R, Spreeuw H, van Herk M, Mans A. Current status of 3D EPID-based in vivo dosimetry in The Netherlands Cancer Institute. *J Phys: Conf Ser* 2015. IOP Publishing.
8. Almond PR, Biggs PJ, Coursey BM, et al. AAPM's TG-51 protocol for clinical reference dosimetry of high-energy photon and electron beams. *Med Phys* 1999;**26**(September (9)):1847–70.
9. Herman MG, Balter JM, Jaffray DA, et al. Clinical use of electronic portal imaging: report of AAPM Radiation Therapy Committee Task Group 58. *Med Phys* 2001;**28**(May (5)):712–37.
10. Kavuma A, Glegg M, Currie G, Elliott A. Assessment of dosimetrical performance in 11 Varian a-Si500 electronic portal imaging devices. *Phys Med Biol* 2008;**53**(23):6893.
11. Commission IE. *Medical electrical equipment: medical electron accelerators-functional performance characteristics*. International Electrotechnical Commission; 1989.
12. Halabi T, Faddegon B. Practical quantitative measurement of graticule misalignment relative to collimator axis of rotation. *J Appl Clin Med Phys* 2010;**11**(4).
13. Klein EE, Hanley J, Bayouth J, et al. Task Group 142 report: quality assurance of medical accelerators. *Med Phys* 2009;**36**(9):4197–212.
14. Grządziel A, Smolińska B, Rutkowski R, Ślosarek K. EPID dosimetry – configuration and pre-treatment IMRT verification. *Rep Pract Oncol Radiother* 2007;**12**(6):307–12.
15. Sukumar P, Padmanaban S, Jeevanandam P, Kumar SS, Nagarajan V. A study on dosimetric properties of electronic portal imaging device and its use as a quality assurance tool in Volumetric Modulated Arc Therapy. *Rep Pract Oncol Radiother* 2011;**16**(6):248–55.
16. Winkler P, Hefner A, Georg D. Implementation and validation of portal dosimetry with an amorphous silicon EPID in the energy range from 6 to 25 MV. *Phys Med Biol* 2007;**52**(15):N355.
17. Tyler M, Vial P, Metcalfe P, Downes S. Clinical validation of an in-house EPID dosimetry system for IMRT QA at the Prince of Wales Hospital. *J Phys: Conf Ser* 2013. IOP Publishing.
18. Greer PB, Popescu CC. Dosimetric properties of an amorphous silicon electronic portal imaging device for verification of dynamic intensity modulated radiation therapy. *Med Phys* 2003;**30**(7):1618–27.
19. Fredh A, Korreman S, af Rosenschöld PM. Automated analysis of images acquired with electronic portal imaging device during delivery of quality assurance plans for inversely optimized arc therapy. *Radiother Oncol* 2010;**94**(2):195–8.